an increase in blood pressure in conscious rats (Fig. 4). After oral administration of OPC-21268 (10 mg/kg), the vasoconstriction induced by exogenous AVP was inhibited in a time-dependent manner (Fig. 4A). The inhibitory effect of OPC-21268 was dose-dependent, and the effect lasted for more than 8 hours at 30 mg/kg. The 50% inhibition dose ($ID_{50}$) for AVP-induced vasoconstriction, was estimated as 2 mg/kg. These data suggest that OPC-21268 antagonized V1 receptors after oral and i.v. administration.

We have described an orally effective, nonpeptide vasopressin V1 receptor antagonist, OPC-21268, that is more than 1000 times as selective for V1 receptors as for V2 receptors. It is expected that OPC-21268 will be a useful probe for studying the physiological or pathophysiological role of AVP.

REFERENCES AND NOTES


1. W. A. Anderson and E. Brown, *Biochim. Biophys. Acta* 67, 674 (1963); J. Bockart, C. Roy, R. Rajerison, S. Jard, *J. Biol. Chem.* **248**, 5922 (1973).
2. M. E. M. Tolbert, A. C. White, K. Aspry, J. Cutts, J. N. Fain, *J. Biol. Chem.* **255**, 1938 (1980); M. J. Berridge and R. F. Irvine, *Nature* **212**, 315 (1984).
3. M. Manning, J. Lowbrige, C. T. Stier, J. Haldar, W. H. Sawyer, *J. Med. Chem.* **20**, 1228 (1977); M. Kruszynski, *ibid.* **23**, 364 (1980); M. Manning, B. Lammek, A. M. Kolodziejczyk, J. Seto, W. H. Sawyer, *ibid.* **24**, 701 (1981); W. H. Sawyer *et al.*, *Science* **212**, 49 (1981); M. Manning and W. H. Sawyer, *J. Lab. Clin. Med.* **114**, 617 (1989).
4. T. Nakamura, A. Tomomura, C. Noda, M. Shimoji, A. Ichihara, *J. Biol. Chem.* **258**, 9283 (1983); T. Nakahara *et al.*, *ibid.* **253**, 3211 (1978).
5. O. H. Lowry, N. J. Rosebrough, A. L. Farr, R. J. Randall, *ibid.* **193**, 265 (1951).
6. Y. Yamamura *et al.*, unpublished data.
7. J. Gillespie and T. C. Muir, *Br. J. Pharmacol. Chemother.* **30**, 78 (1967); J. T. A. Knape and P. A. van Zwieten, *Arch Int. Pharmacodyn. Ther.* **291**, 142 (1988).


8. We thank Y. Orita of Osaka University for suggestions and encouragement during this study and N. Taira of Tohoku University for review and criticism of the manuscript.

19 October 1990; accepted 1 February 1991


# Uncoupling of the Spectrin-Based Skeleton from the Lipid Bilayer in Sickled Red Cells


SHIH-CHUN LIU, LAURA H. DERICK, SEN ZHAI, JIRI PALEK



**The distribution of spectrin and band 3 in deoxygenated reversibly sickled cells was visualized by immunofluorescence and immunoelectron microscopy. Antibodies against band 3, the major lipid-associated transmembrane protein, labeled the entire cell body, including the entire length of the long protruding spicule, whereas antibodies against spectrin labeled only the cell body and the base region of the spicules. The results suggest that the formation of long spicules during sickling is associated with a continuous polymerization of hemoglobin S polymers, presumably through gaps in the spectrin-actin meshwork, and a subsequent uncoupling of the lipid bilayer from the submembrane skeleton.**


IN ERYTHROCYTES FROM PATIENTS with sickle cell anemia, intracellular hemoglobin S (HbS) undergoes polymerization under conditions of low oxygen tension to produce sickle-shaped erythrocytes, often with long spicules protruding from the cell surface. In reversibly sickled cells (RSCs), these abnormalities disappear upon reoxygenation. In a subpopulation of erythrocytes, the irreversibly sickled cells, the abnormal shape persists after reoxygenation, despite the absence of polymerized hemoglobin in the cells (*1*). During repeated cycles of deoxygenation and reoxygenation, sickled cells shed as vesicles the part of the plasma membrane that almost completely lacks the skeletal proteins spectrin and actin (*2*). The mechanism of this membrane loss after repeated sickling is not clear. One possibility is that the lipid bilayer is uncoupled from the underlying membrane skeleton in the long protrusions. The disruption of the membrane skeleton–lipid interaction in the spicules may lead to a subsequent loss of membrane material from the sickle-shaped erythrocytes upon reoxygenation. We used the immunofluorescence and immunoelectron microscopy techniques to study the distribution of spectrin, a major skeletal protein, and band 3, a major lipid-associated, transmembrane protein, in cells undergoing deoxygenation-induced sickling in vitro.

Antibodies against band 3 labeled the whole cell body, including the entire length of the spicules. In contrast, spectrin antibodies labeled only the cell body and the base region of the spicules, but not the length of the spicules, including the tips (Fig. 1). A marked reduction in staining intensity by spectrin antibodies in the spicule regions, as compared to that in the cell body, was consistently detected, regardless of the concentrations of spectrin antibodies used. Preimmune sera or secondary antibody alone did not label the cells.

The presence of band 3, but not spectrin, in the membrane regions laminating the long spicules of the deoxygenated sickle-shaped cells was further verified by immunoelectron microscopy. Secondary antibodies conjugated with colloidal gold (15-nm diameter) were used to label spectrin and

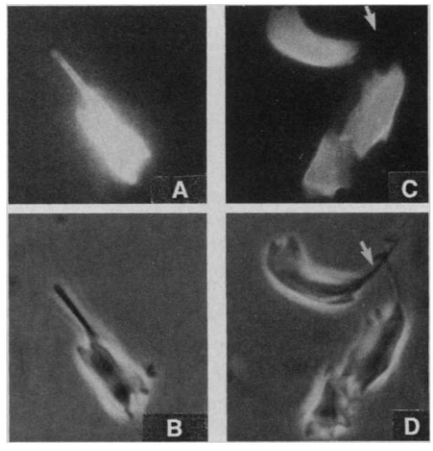


**Fig. 1.** Immunofluorescence labeling of band 3 (**A** and **B**) and spectrin (**C** and **D**) in deoxygenated RSCs. RSCs were isolated from patients with homozygous sickle cell disease (*11*). A 2% RSC suspension in phosphate-buffered saline (PBS) was incubated at 37°C for 1 hour under deoxygenated conditions with humidified $N_2$ to induce cell sickling. After incubation, cells were fixed at 25°C for 30 min with glutaraldehyde (0.1 to 0.2%, final concentration) in PBS that had been previously deoxygenated. Cells were then permeated by brief treatment (25°C, 5 min) with 0.5% Triton X-100 in PBS and washed with 0.05% Tween 20 in PBS. Affinity-purified antispectrin or antiband 3 antibodies in PBS with 1% bovine serum albumin and 0.05% Tween 20 were added to the cell sediment, and incubation proceeded with mild shaking for 1 hour at 25°C. Cells were then washed and incubated at 25°C for 1 hour with a second antibody solution of fluorescein-conjugated goat antirabbit immunoglobulin (Ig) G (Cappel, Malvern, Pennsylvania). Control samples were incubated with the secondary antibody but without the primary antibody to ensure that the secondary antibody did not cause any artificial background. The immunolabeled sickled cells were washed and examined by phase contrast (B and D) or fluorescence light (A and C) microscopy. The results show that the long spicules of deoxygenated RSCs were labeled by antibodies to band 3, but not by antibodies to spectrin (arrows).


Division of Hematology-Oncology and Departments of Biomedical Research and Medicine, St. Elizabeth's Hospital, Tufts University School of Medicine, Boston, MA 02135.

**Table 1.** Distribution of antiband 3 and antispectrin antibodies on spicules of deoxygenated sickled cells.

| Target of antibody | Region of spicule examined | Gold particles (no. ± SD per $\mu m^2$) | No. of spicules analyzed | Total surface area analyzed ($\mu m^2$) |
|---|---|---|---|---|
| Band 3 | Tip | 55.8 ± 9.3 | 4 | 4.7 |
| | Base | 58.8 ± 12.4 | 4 | 4.7 |
| Spectrin | Tip | 1.4 ± 1.2 | 4 | 12.7 |
| | Base | 43.3 ± 15.8 | 4 | 2.7 |

band 3 indirectly in the long spicules of deoxygenated RSCs and were visualized by transmission electron microscopy without chemical staining of the RSCs. Band 3 immunogold label was seen on both the main cell body and the entire membrane spicule (Fig. 2A). The presence of HbS polymers in the spicules was also evident on the negatively stained samples (Fig. 2B). In contrast, spectrin immunogold label was seen only on the membrane region covering the cell body and the base regions of the spicules, but not on the rest of the protruding spicule (Fig. 2C). The number of spectrin immunogold particles per unit surface area measured in the tip region of the spicule was less than 4% of that of the base region of the spicule (Table 1). No significant quantitative difference of band 3 labeling was evident between the tip and base regions of the long protrusion (Table 1). The presence of band 3, but not spectrin, in the tips of the spicules, together with the finding of polymerized HbS in the spicules, suggests that HbS polymers in the deoxygenated RSCs penetrate the membrane skeleton near the base region of the spicule and uncouple the lipid bilayer from the skeleton in the process of forming long spicules.

Furthermore, we analyzed the neck region of the spicule by the immunogold labeling and the scanning electron microscopy techniques to clarify the distribution of spectrin at the site of the lipid bilayer-skeleton separation (Fig. 3). No labeling was apparent beyond the neck region, where the narrow spicules extended out. Immunogold-labeled antiband 3 antibodies, however, labeled the entire membrane spicule (*3*). The absence of spectrin in the long spicules of deoxygenated sickle-shaped cells suggests that spicule HbS polymerized through gaps in the spectrin-actin meshwork and caused a herniation of the membrane lipid bilayer, followed by an uncoupling of the lipid bilayer from the submembrane skeleton (Fig. 4).

This disruption of the spicule membrane skeleton-lipid interaction may lead to a subsequent loss of membrane material from the sickle-shaped erythrocytes. Upon reoxygenation in vitro, spicules became round and detached from the body of the erythrocyte (*4*) in the form of spectrin-free microvesicles or microvesicle chains that contained HbS (*2, 5*). Spectrin-free microvesicles have been detected in the plasma of patients with sickle cell anemia, suggesting that the loss of spicules from sickled cells may also occur in vivo (*2*).

The loss of membrane material in the form of spectrin-free microvesicles has been observed in normal red cells after a variety of conditions such as calcium uptake, depletion of intracellular adenosine triphosphate stores, heating, or storage (*6, 7*). In normal

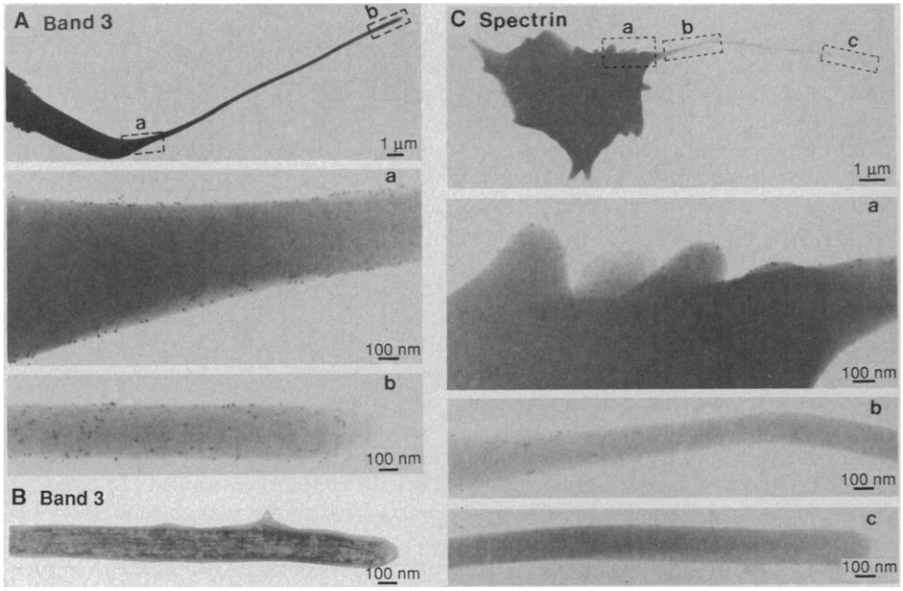


**Fig. 2.** Transmission electron micrographs of band 3 and spectrin immunogold-labeled RSCs. Deoxygenated sickled cells were fixed, permeated, and incubated with rabbit antispectrin or antiband 3 antibodies as described in Fig. 1, except that the incubation with antibodies was carried out at 0°C for 16 hours. Cells were washed and then incubated at 0°C for 16 to 24 hours with goat antirabbit IgG coupled to 15-nm gold particles (Janssen, Beerse, Belgium), washed again, applied onto thin carbon-coated copper grids (1000 mesh), air-dried, and then examined by transmission electron microscopy. (**A**) Band 3 labeling. High magnifications of regions a and b are also shown. (**B**) Tip of the long spicule labeled with antiband 3 antibodies and then negative-stained with uranyl acetate (1%). HbS polymers (16-nm thickness) were detected in the spicule. (**C**) Spectrin labeling. High magnifications of regions a, b, and c are also shown. Spectrin, but not band 3, is absent from the long spicule.

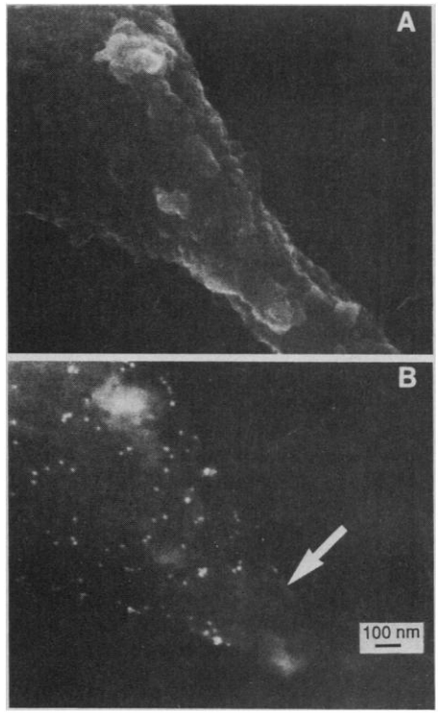


**Fig. 3.** Scanning electron micrographs of the neck region of the long spicule labeled with antispectrin immunogold. The immunogold-labeled cells were fixed in 0.25% glutaraldehyde in PBS for 2 hours at 0°C, dehydrated, and critical-point dried (*12*). Samples were coated with a thin layer of carbon and examined by the scanning electron microscopy technique on a JEOL JSM 840 scope with an accelerating voltage of 15 kV. (**A**) Secondary electron image. (**B**) Backscattered electron image of the same field as in (A). Immunogold-labeled antispectrin antibodies labeled the proximal end of the neck, but not more distal parts of the neck and spicule. Arrow indicates the neck.

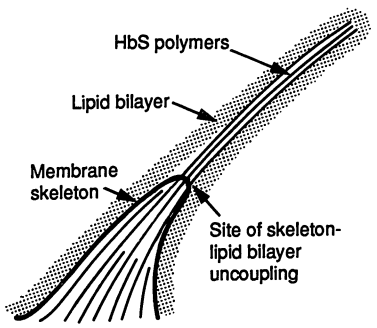


**Fig. 4.** Model of the long spicule in the deoxygenated sickled cell shows HbS polymers penetrating the membrane skeleton and the lipid bilayer uncoupling from the skeleton.

red cell ghosts that are induced at physiological salt concentrations to undergo transformation into echinocytes, the lipid bilayer becomes uncoupled from the skeleton (*8*), probably because of imbalances between the lipid and skeleton surface areas in the spicules of echinocytic cells. In contrast, the uncoupling of the lipid bilayer in the spicules of deoxygenated sickled cells is passively induced by HbS polymerization through gaps in the skeletal network, not by imbalances in lipid and skeleton surface areas. Lipid bilayers detached from their underlying spectrin skeletons are mechanically unstable and are prone to release from the cell body.

It is possible that the membrane in the spicule region suffers additional damage as a result of the lack of an underlying skeletal network, such as the loss of lipid asymmetry across the lipid bilayer (*9*), which has been demonstrated in RSC spicules (*5, 9*), and an increased leakage of intracellular and extracellular cations across the membrane (*10*). Future studies are needed to determine whether or not the increased cation leakages also occur in the spicules of these deoxygenated RSCs.

REFERENCES AND NOTES

1. J. F. Bertles and J. Dobler, *Blood* **33**, 884 (1969).
2. D. Allan, A. R. Limbrick, P. Thomas, M. P. Westernman, *Nature* **295**, 612 (1982).
3. S. C. Liu, L. H. Derick, J. Palek, unpublished data.
4. W. N. Jensen and L. S. Lessin, *Semin. Hematol.* **7**, 409 (1970).
5. P. F. H. Franck *et al.*, *J. Clin Invest.* **75**, 183 (1985).
6. D. Allan and P. Thomas, *Biochem. J.* **198**, 433 (1981).
7. P. Ott *et al.*, *Biochim. Biophys. Acta* **641**, 79 (1981); H. U. Lutz, S. C. Liu, J. Palek, *J. Cell Biol.* **73**, 548 (1977); W. T. Coakly, A. J. Bater, J. O. T. Deeley, *Biochim. Biophys. Acta* **512**, 318 (1978); M. G. Rumsby, J. Trotter, D. Allan, R. H. Michell, *Biochem. Soc. Trans.* **5**, 126 (1977); G. M. Wagner, D. T. Y. Chiu, M. C. Yee, B. H. Lubin, *J. Lab. Clin. Med.* **108**, 315 (1986).
8. S. C. Liu, L. H. Derick, M. A. Duquette, J. Palek, *Eur. J. Cell Biol.* **49**, 358 (1989).
9. P. F. H. Franck *et al.*, *J. Biol. Chem.* **258**, 8435 (1983); E. Middelkoop *et al.*, *Biochim. Biophys. Acta* **937**, 281 (1988).
10. D. C. Tosteson, E. Shea, R. C. Darling, *J. Clin. Invest.* **31**, 406 (1952); L. R. Berkowitz and E. P. Orringer, *Am. J. Physiol.* **249**, C208 (1985); C. H. Joiner, O. S. Platt, S. E. Lux, *J. Clin. Invest.* **78**, 1487 (1986); C. Brugnara, H. F. Bunn, D. C. Tosteson, *Science* **232**, 388 (1986); M. Canessa, M. E. Fabry, R. L. Nagel, *Blood* **70**, 1861 (1987); R. M. Bookchin and V. L. Lew, *J. Physiol.* **312**, 265 (1981); C. H. Joiner, A. Dew, D. L. Ge, *Blood Cells* **13**, 339 (1988); N. Mohandas, M. E. Rossi, M. R. Clark, *Blood* **68**, 450 (1986).
11. J. Palek, S. C. Liu, P. A. Liu, in *Erythrocyte Membranes: Recent Clinical and Experimental Advances*, W. C. Kruckenberg, J. W. Eaton, G. J. Brewer, Eds. (Liss, New York, 1978), p. 75.
12. H. Ris, *J. Cell Biol.* **100**, 1474 (1985).
13. We thank V. Robertson (JEOL USA) for obtaining scanning electron micrographs of immunogold-labeled sickled cells; D. Howard for rabbit immunization; J. Zhou and P. Nichols for antibody purification; and G. Maitino and J. Joos for preparation of the manuscript. Supported by the Robert J. Kleberg, Jr., and Helen C. Kleberg Foundation and by grants from NIH (HL-27215, 37462, and 15157-7) (to J.P.).

21 August 1990; accepted 30 January 1991

# Regulation of Ras-GAP and the Neurofibromatosis-1 Gene Product by Eicosanoids

JIA-WEN HAN,* FRANK MCCORMICK, IAN G. MACARA*†

**Ras-GAP (GTPase activating protein) is a regulatory protein that stimulates the intrinsic guanosine triphosphatase (GTPase) activity of the proto-oncogene product p21$^{ras}$. A domain of the neurofibromatosis gene product (NF1) that has sequence similarity to the catalytic domain of Ras-GAP and to yeast IRA gene products also has a specific stimulatory activity toward p21$^{ras}$ GTPase. Arachidonic acid and phosphatidic acid inactivate GAP, but no agents have been identified that stimulate GAP and thereby switch p21$^{ras}$ off. With the use of recombinant Ha-c-Ras and Ras-GAP, NF1, and GAP catalytic domains, it was found that prostaglandins $PGF_{2\alpha}$ and $PGA_2$ stimulated Ras-GAP and that prostacyclin $PGI_2$ inhibited Ras-GAP. The stimulatory effect of $PGF_{2\alpha}$ was saturable and structure-specific and competed with the inhibitory effect of arachidonic acid. Arachidonic acid also inhibited the catalytic activity of NF1, but prostaglandins were not stimulatory. These results suggest a mechanism for the allosteric control of Ras function through the modulation of arachidonate metabolism.**

THE *ras* GENE PRODUCTS ARE 21-KD guanosine triphosphate (GTP)–binding proteins that act as molecular switches to control cell growth (*1*). Guanine nucleotide exchange factors can convert p21$^{ras}$ to the active ("on") state, and a slow, intrinsic GTPase activity returns p21$^{ras}$ to the inactive ("off") state (*2*). GAP accelerates the rate of GTP hydrolysis by p21$^{ras}$ (*3*). The neurofibromatosis gene has sequence similarity to the mammalian *ras*-GAP and yeast IRA genes (*4*), and the catalytic domain of NF1 exhibits GAP-like activity (*5*). Both Ras-GAP and NF1 are commonly expressed (*3, 4*), and the question arises as to whether or not they are differentially controlled. Tyrosine kinases phosphorylate and may indirectly inactivate GAP (*6*). Moreover, certain lipids that are generated in response to mitogenic stimuli, particularly arachidonic acid and phosphatidic acid, also bind to and inactivate GAP (7). Additionally, a cytosolic protein has been described that inhibits p21$^{ras}$ GTPase activity (7). Either of these inhibitory mechanisms would increase the proportion of p21$^{ras}$ in the on state, but no mechanisms have been identified that stimulate GAP and switch p21$^{ras}$ off.

Cyclooxygenase, which catalyzes the synthesis of prostaglandins from arachidonic acid, is an early-immediate gene product induced by growth factors, cytokines, and certain oncogenes (*8*). Because arachidonic acid inhibits Ras-GAP, we reasoned that other metabolites of arachidonate might also regulate the interaction of Ras and GAP or NF1. Therefore, we studied the effect of prostaglandins on recombinant Ha-c-Ras and recombinant GAP (*9*). The proportion of $^{32}$P-labeled GTP hydrolysed over time was estimated either by direct filter binding ([$\gamma$-$^{32}$P]GTP) or by filter binding, extraction, and separation of the nucleotides ([$\alpha$-$^{32}$P]GTP) by thin-layer chromatography (*10*) (Fig. 1). In the absence of GAP, none of the prostaglandins tested altered the basal GTPase activity of p21$^{ras}$. However, both $PGF_{2\alpha}$ and $PGE_2$ increased the effect of GAP on p21$^{ras}$ GTP hydrolysis, and prosta-

J.-W. Han and I. G. Macara, Environmental Health Sciences Center, Department of Biophysics, University of Rochester Medical Center, Rochester, NY 14642.
F. McCormick, Department of Molecular Biology, Cetus Corporation, Emeryville, CA 94608.

*To whom correspondence should be addressed.
†Address from 1 June 1991 will be Department of Pathology, University of Vermont, Burlington, VT 05405.